Catalysis Today 175 (2011) 558–567

Contents lists available at ScienceDirect

Catalysis Today

journal homepage: www.elsevier.com/locate/cattod

Study on the catalytic reaction mechanism of low temperature oxidation of CO over Pd–Cu–Cl_x/Al_2O_3 catalyst

Yuexin Shen, Guanzhong Lu*, Yun Guo, Yanqin Wang, Yanglong Guo, Xueqing Gong

Key Laboratory for Advanced Materials and Research Institute of Industrial Catalysis, East China University of Science and Technology, Shanghai 200237, PR China

ARTICLE INFO

Article history:
Received 19 October 2010
Received in revised form 5 February 2011
Accepted 16 March 2011
Available online 22 April 2011

Keywords:
Low temperature CO oxidation
Pd–Cu–Cl_x catalyst
Coordination-impregnation method
Catalytic reaction mechanism
Catalyst preparation

ABSTRACT

The Pd–Cu–Cl_x/Al_2O_3 catalysts were prepared by an NH_3 coordination-impregnation (CI) method in water and organic solvents, and exhibited much higher activity for CO oxidation than the catalyst prepared by conventional wet impregnation (WI) method. Their chemical and physical properties were characterized by X-ray diffraction (XRD), transmission electron microscopy (TEM), temperature-programmed reduction (TPR), X-ray photoelectron spectroscopy (XPS) and *in situ* diffuse reflectance infrared Fourier transform spectroscopy (DRIFTS). The results show that in the process of preparing the catalysts by CI, different solvents affect obviously their catalytic performance and isopropanol is the most suitable solvent among water, ethanol, acetone and isopropanol. The CO oxidation over Pd–Cu–Cl_x/Al_2O_3 catalyst (CI) can be accelerated remarkably with an increase of H_2O concentration in the reactant gas, and it is weakly dependent on the CO and O_2 concentrations. Compared with the catalyst prepared by WI, the catalyst prepared by CI possesses the higher dispersion and lower-temperature reducibility of copper phase, much more active Cu^{2+} species, and easier re-oxidation of Cu^+. The Pd^+ active site on the catalyst (CI) is more active than Pd^{2+} on the catalyst (WI), and the rate-determining step is the re-oxidation of Pd^0 to Pd^+ by Cu^{2+} on the catalyst (CI) instead of the re-oxidation of Cu^+ to Cu^{2+} by O_2 on the catalyst (WI).

1. Introduction

Low temperature CO oxidation is a very important research subject all the time, because of its importance for practical applications and academic studies in the catalysis field, such as air purification, CO leak detection and automotive emission control [1–4]. Among the oxide catalysts for the CO oxidation, the hopcalite catalyst (a mixture of manganese and copper oxides) and Co_3O_4 are active at room temperature, especially Co_3O_4 catalyst that is active even at −77 °C, but both of them deactivate severely in the presence of trace amount of moisture [5–8]. The moisture level in air sometimes is near to saturated vapor, so their applications are now restricted. Since the pioneering work by Haruta [9], gold-based catalysts show the exceptional activity for low temperature CO oxidation and the good stability under moisture [10,11]. However gold-based catalysts also suffer several unsolved defects, for example, deactivation in the storage and the indoor light, sensitiveness to halogen-including compounds, high cost of gold [12–15]. Therefore the high property catalysts that are impervious to chloride ions and moisture, stable in both the reaction feed and storage are extremely desirable to commercial applications.

Supported $PdCl_2$–$CuCl_2$ catalyst has been used to produce dimethyl carbonate, diethyl carbonate and acetaldehyde [16–19]. It has also been reported to be a stable and active catalyst for CO oxidation even in the presence of organic halogen compounds and large amounts of moisture in the feed [20–22]. These advantages make supported $PdCl_2$–$CuCl_2$ catalyst become a promising catalyst for CO oxidation in the presence of water and halogen compounds at low temperature. However, the supported $PdCl_2$–$CuCl_2$ catalysts are less active compared with gold-based catalysts, and a large amount of research works was done for improving their catalytic activities. For instance, adding $Cu(NO_3)_3$ as a promoter in supported Pd catalyst can enhance its catalytic activity [22]. Park and Lee [23] tested the effects of different Cu precursors, such as $Cu(OH)_2$, $Cu(CH_3COO)_2$, and $CuCO_3$–$Cu(OH)_2$ and their mixtures with $CuCl_2$ on the catalytic performance of Pd, and found that $Cu(NO_3)_2$ was the most appropriate Cu precursor. Lee et al. [24] investigated the effects of different supports on the performances of Pd–Cu bimetallic complexes, and found that hydrophobic supports were superior to hydrophilic supports. The studies [21,25] further show that the catalyst supported on hydrophobic carbon has higher activity than one on hydrophilic alumina. Park and Lee [22] examined the effect of pretreatments of active carbon support on the catalytic performance, and their results showed that carbon support pretreated with HNO_3 can promote the catalytic activities of Pd–Cu bimetallic complexes.

---

* Corresponding author. Fax: +86 21 64253824.
E-mail address: gzhlu@ecust.edu.cn (G. Lu).

0920-5861/$ – see front matter © 2011 Elsevier B.V. All rights reserved.
doi:10.1016/j.cattod.2011.03.042

There have been a number of research works on the catalytic active sites and surface reactions over supported $PdCl_2$–$CuCl_2$ catalysts. Using an X-ray absorption fine structure (XAFS), Lee et al. [26,27] examined the $PdCl_2$–$CuCl_2/Al_2O_3$ catalysts and found that the active palladium phase was Pd^{2+} species containing Cl and carbonyl ligands. And any direct interaction of Pd–Pd or Pd–Cu was not observed. The active copper phase was suggested to be solid $Cu_2Cl(OH)_3$ particles, which was the indispensable redox partner of palladium species in the Wacker chemistry. Choi and Vannice [25,28] investigated the mechanism of CO oxidation by the kinetics and infrared spectroscopy, and they suggested that the active species on the catalyst surface were PdClCO and CuClCO, and possibly the Pd–Cu complex. Park et al. [29,30] thought that $Cu_2Cl(OH)_3$ was the most active phase, and the formation of $Cu_2Cl(OH)_3$ was based on basic hydroxyl groups on the surface of support, irrespective of combination with the palladium species.

In order to improve the performances of $PdCl_2$–$CuCl_2$ catalysts for the CO oxidation, the previous works mainly focused on adding different additives or searching for a proper support. We have used the coordination-impregnation (CI) method to prepare Al_2O_3 supported Pd–Cu–Cl_x catalysts that exhibit the excellent activity for low temperature CO oxidation [31]. Herein, we have systematically studied the relationship between the preparation method and high catalytic performance of Pd–Cu–Cl_x catalysts by the kinetics parameters testing, XRD, TEM, TPR, XPS and *in situ* DRIFTS. It is found that the Pd^+ species is the active site for CO oxidation over the catalysts prepared by CI method, and the rate-determining step is the re-oxidation of Pd^0 by Cu^{2+} in the Pd–Cu–Cl_x/Al_2O_3 catalyst (CI) instead of the re-oxidation of Cu^+ to Cu^{2+} by O_2 in the conventional supported $PdCl_2$–$CuCl_2/Al_2O_3$ catalysts.

2. Experimental

2.1. Materials

$CuCl_2$ (AR), 25% ammonia solution and all organic reagents (ethanol, isopropanol and acetone, AR) were from Sinoharm Chemical Reagent Co., Ltd. (SCRC); $PdCl_2$ (AR) from Heraeus Materials Technology Shanghai Ltd.; Al_2O_3 (WHA-204, BET surface area of 194 m^2/g) from Wen-Zhou Jingjing Aluminum Ltd.

2.2. Catalysts preparation

The supported 1.7 wt.%Pd–3.3 wt.%Cu–Cl_x/Al_2O_3 catalysts were prepared by an NH_3 coordination-impregnation (CI) method with different solvents [31]. Weighed $PdCl_2$ and $CuCl_2$ were dissolved in 2 ml 25% ammonia solution under ultrasonic at room temperature, and this mixed aqueous solution of $PdCl_2$ and $CuCl_2$ was diluted to 8 ml with de-ionized water or the organic reagents (such as ethanol, acetone and isopropanol). Then 1 g Al_2O_3 was impregnated in this solution. After being aged for 24 h, the catalyst was dried at room temperature and calcined at 300 °C for 4 h. The Pd–Cu–Cl_x/Al_2O_3 catalyst prepared by the CI method is denoted as PC-CI. In the preparation of catalyst, water, acetone, ethanol, or isopropanol were used as the solvent respectively, the catalyst was denoted as PC-CIw, PC-CIa, PC-CIe, and PC-CIi.

The 1.7 wt.%Pd–3.3 wt.%Cu–Cl_x catalyst was prepared by the wet impregnation (WI) method [23–31] with water as a solvent and dried at room temperature, denoted as PC-WI.

2.3. Catalysts characterization

The powder X-ray diffraction (XRD) pattern of sample was performed on a Brook D8 focus diffraction spectrometer with Cu Kα radiation at room temperature. The average crystalline size of sample was determined by the Scherrer formula based on the diffraction peak broadening. The transmission electron microscopy (TEM) images of catalyst were obtained on a TECNAl 20S-TWIN. The X-ray photoelectron spectroscopy (XPS) spectra were obtained at 298 K on a Thermo ESCALAB 250 spectrometer with Al Kα (1486.6 eV) radiation as the excitation source. All binding energies (BE) were determined with respect to the C1s line (284.8 eV) originating from adventitious carbon. The powder samples were pressed into self-supporting disks loaded in the sub-chamber, and evacuated for 4 h.

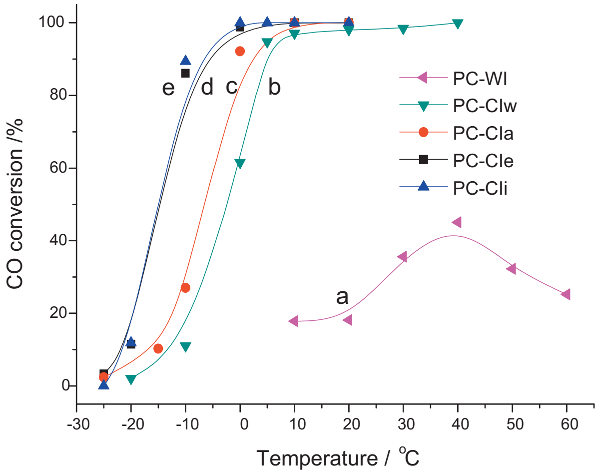

Fig. 1. Catalytic activity of (a) PC-WI, (b) PC-CIw, (c) PC-CIa, (d) PC-CIe and (e) PC-CIi for CO oxidation. (1500 ppm CO and ~6000 ppm water in air, WHSV 15,000 ml g^{-1} h^{-1}).

H_2-temperature programmed reduction (H_2-TPR) was performed in a quartz U-tube with 100 mg catalyst. The catalysts prepared by CI were firstly pretreated in N_2 flow at 300 °C for 1 h, and cooled down to room temperature; the catalysts prepared by WI were pretreated in N_2 flow at room temperature for 1 h. The reduction gas was consisted of 5% H_2/N_2 (45 ml/min). The heating rate was 10 °C/min. The uptake amounts of H_2 were measured by a thermal conductivity detector (TCD), which was calibrated by the quantitative reduction of CuO to the metallic copper.

Diffuse reflectance infrared Fourier transform spectroscopy (DRIFTS) of CO adsorbed on the catalyst was measured on a Nicolet Nexus 670 spectrometer equipped with a MCT detector, and the sample cell was fitted with ZnSe windows and a heating chamber can be heated up to 600 °C. The DRIFTS spectra obtained were saved in Kubelka–Munk unit with a resolution of 4 cm^{-1} and 64 scans. The PC-WI sample was pretreated in a He (99.999%) flow of 50 ml/min at room temperature for 1 h and the PC-CI catalysts were pretreated in a He flow at 300 °C for 1 h, and then cooled down to 25 °C and the background spectrum in a He flow was acquired. (1) After the mixture gases of 0.15% CO + O_2 (0%, 5%, 10%, and 20%) + balanced He with 50 ml/min flowed through the sample cell for 30 min, the spectra were taken down at 25 °C; (2) ~6000 ppm H_2O was added in the mixture gases (1) above, and the spectra were taken down again at 25 °C; (3) CO was removed from the mixture gases (2) above, and the spectra were also taken down at 25 °C.

2.4. Testing of the catalytic activity and kinetic parameters

The activities of catalysts for CO oxidation were measured in a (Ø5 mm) quartz U-tube reactor, and 0.2 g catalyst (20–40 mesh) was used and a glass wool was plugged in both sides of catalyst. The feed gas of 1500 ppm CO in air at a flow rate of 50 ml/min was directly through a water vapor saturator immersed in ice-water bath, and then flowed into the reactor. The water concentration in the feed gas was ~6000 ppm. Changing the temperature of cold

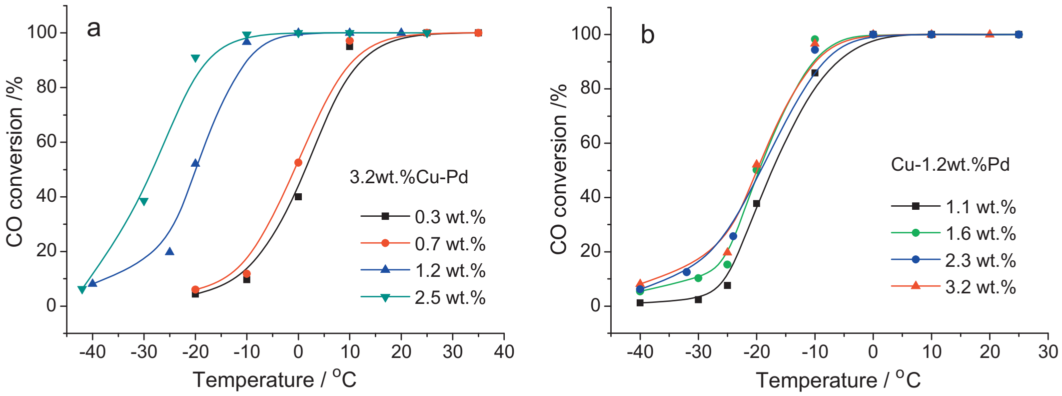

Fig. 2. Effects of (a) Pd and (b) Cu loadings on the activity of PC-Cli for CO oxidation. (Pd and Cu loadings were measured by ICP-AES instrument (Varian 710); 1500 ppm CO and ~6000 ppm water in air, WHSV 15,000 ml g^{-1} h^{-1}).

trap can adjust the water concentration in the feed gas. After the steady operation for 10 min, the activity of catalyst was tested. The reactants and products were analyzed by an on-line gas chromatograph equipped with a column packed with carbon molecular sieve, a methanator and a FID. The minimum detection level of CO concentration was 1 ppm. The reaction temperature was controlled as follows: below room temperature was obtained by using ethanol/liquid nitrogen mixture in a vacuum bottle, and above room temperature was achieved by using warm water bath.

In the measurement of kinetic parameters, the reaction temperature was 20 °C, the reactant gas consisted of CO of 700–3000 ppm, O_2 of 2–20%, H_2O of 400–6000 ppm balanced with N_2, and the hourly gas space velocity was 2×10^5–9×10^5 ml g^{-1} h^{-1}. The conversion of CO was adjusted to below 15% in order to calculate the reaction rates under different reaction conditions. The reaction rates were obtained after the reaction run for 30 min.

3. Results and discussion

3.1. Effect of preparation method on the catalytic activity

Fig. 1 shows the effects of different preparation methods on the catalytic activity of 1.7 wt.%Pd–3.3 wt.%Cu–Cl_x/Al_2O_3 (PC) for CO oxidation. The CO conversion over PC-WI (Fig. 1a) at 40 °C reaches a maximum of ~40%, and then decreases with an increase in the reaction temperature, due to the loss of chlorine and water from the catalyst surface at high temperature [21,30,32]. The CO conversion over PC-CIw increases remarkably with a temperature rise and reaches to 100% at 40 °C. When organic reagents were used as solvents in the catalyst preparation, the catalytic activity can be improved obviously. PC-CIi prepared by using isopropanol as a solvent is the most excellent one among the catalysts prepared by CI method, the complete conversion temperature of CO (T_{100}) is 0 °C and even at −10 °C ~90% CO conversion can be obtained. The activity of PC-CIe is slightly lower than that of PC-CIi, and higher than that of PC-CIa. For PC-CIe catalyst, its T_{100} is 10 °C and lower than T_{100} over PC-CIw. Compared with the PC-WI catalyst prepared by WI method, PC-CI catalysts prepared by CI method present much higher activities for low temperature oxidation of CO.

Based on the results above, the PC-CIi catalyst prepared by CI with isopropanol solvent is used in the following tests unless stated otherwise.

3.2. Effect of Pd and Cu loadings on the catalytic activity

The effects of Pd and Cu loadings on the catalytic activity of PC-CIi for the CO oxidation were investigated, and the results are shown in Fig. 2. The results in Fig. 2a show that the catalytic activity of PC-CIi with a fixed Cu loading (3.2 wt.%) is improved gradually with an increase in the Pd loading. When the Pd loading is 0.3 wt.%, T_{100} is 25 °C; when Pd loading is 2.5 wt.%, T_{100} is −10 °C, which indicates Pd species should be the main catalytic active species [20–24]. The effect of Cu loading on the catalytic activity of PC-CIi with a fixed Pd loading (1.2 wt.%) for the CO oxidation is shown in Fig. 2b. It was reported that a high Cu loading was needed for the $PdCl_2$–$CuCl_2$ catalyst in order to maintain its catalytic activity for CO oxidation, and the CO conversion could be increased with an increase in Cu loading as Pd loading was a fixed constant [21–24]. However, the results in Fig. 2b show that the Cu loading has a little influence on the catalytic activity of PC-CIi, for instance, when the Cu loading increases from 1.1 wt.% to 3.2 wt.%, T_{50} is changed only from −17 °C to −20 °C. This is different from the $PdCl_2$–$CuCl_2$ catalyst reported previously. Hence, the PC-CIi catalyst may have the different active sites or the different reaction mechanism for CO oxidation.

3.3. Effect of WHSV on the CO catalytic oxidation

Fig. 3 shows that the CO conversion over PC-CIi as the function of space velocity (WHSV). When a WHSV is below 15,000 ml g^{-1} h^{-1}, the CO conversion is hardly affected by the space velocity. When the space velocity increases, the CO conversions over PC-CIi decrease because the residence time of CO in the catalyst bed decreases with the increase of WHSV, and suitably raising temperature is needed in order to achieve a sufficient conversion of CO at a higher space velocity.

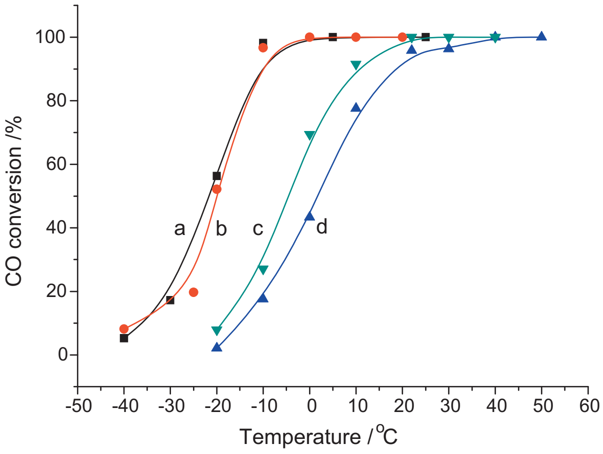

Fig. 3. Catalytic activity of PC-CIi for CO oxidation in a WHSV (ml g^{-1} h^{-1}) of (a) 10,000, (b) 15,000 (c) 20,000 and (d) 30,000. (1500 ppm CO and ~6000 ppm water in air).

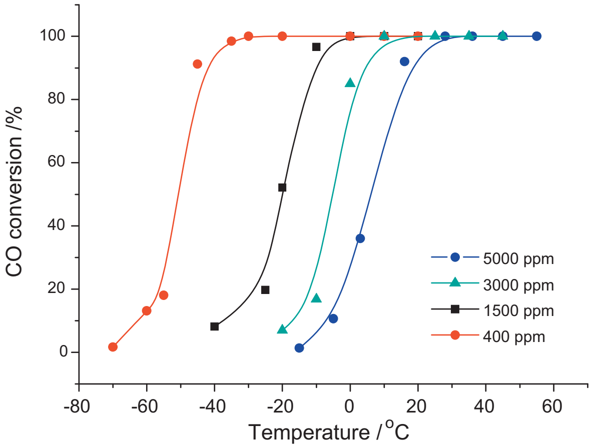

Fig. 4. Effect of CO concentrations on the CO conversion over PC-CIi catalyst. (~6000 ppm water balanced with air, WHSV 15,000 ml g^{-1} h^{-1}).

3.4. Effect of CO concentration on the CO catalytic oxidation

The effect of the CO concentration on the CO conversion over PC-CIi at the space velocity of 15,000 ml g^{-1} h^{-1} was investigated, and the results are shown in Fig. 4. It can be seen that the CO conversion increases (or T_{100} falls) significantly with a decrease in the CO concentration from 5000 to 400 ppm. Using the feed gas with CO concentration of 400 ppm, T_{100} is only −30 °C. When the CO concentration is 1500, 3000 and 5000 ppm, T_{100} is increased to 0 °C, 10 °C and 28 °C, respectively.

3.5. Effect of water in feed gas on the CO catalytic oxidation

Water was considered to be essential for maintaining the high catalytic activity of supported $PdCl_2$–$CuCl_2$ catalyst for the CO oxidation, and it may contribute as a reactant to form CO_2 for the water gas shift reaction [25]. Fig. 5 shows the effect of water on the CO catalytic oxidation over PC-CIi. The results show that, as water feed is stopped, the conversion of CO oxidation falls from 100% to 45% during ~45 min. However, once water is re-fed, the CO conversion recovers quickly. Therefore, the presence of water in feed gas exhibits the prompting effect on the CO oxidation over the PC-CIi catalyst.

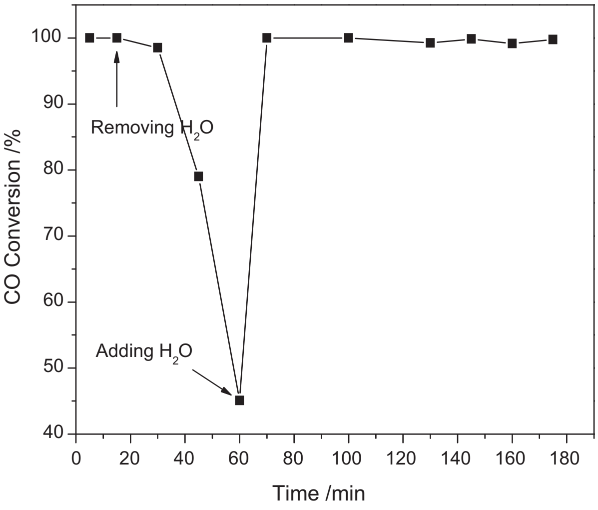

Fig. 5. Effect of water on the CO oxidation over PC-CIi at 25 °C. (1500 ppm CO and ~6000 ppm water in air, WHSV 15,000 ml g^{-1} h^{-1}).

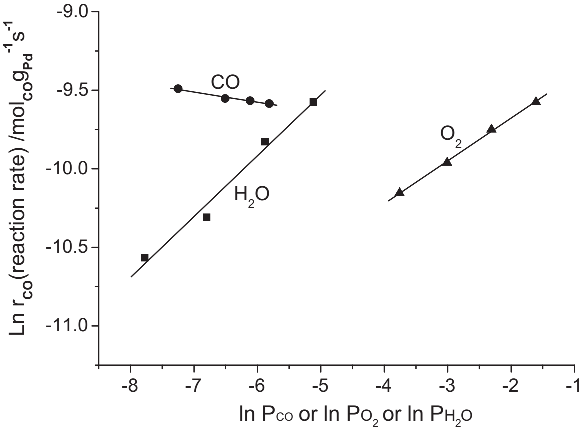

Fig. 6. Reaction rates (r_{CO}) as a function of (●) CO, (▲) O_2 or (♦) H_2O concentration over PC-CIi at 20 °C. (The concentrations of CO, O_2 and H_2O were 700–3000 ppm, 2–20% and 400–6000 ppm respectively. P_{CO}, P_{O2} and P_{H2O}, partial pressures.)

3.6. Testing for kinetic parameters of CO oxidation over PC-CIi catalyst

The reaction orders of CO, O_2 and H_2O were obtained simply by the linear slopes of the reaction rate r_{CO} as a function of CO or O_2 or H_2O concentration over PC-CIi catalyst. When the order of CO (O_2 or H_2O) was tested, the CO (O_2 or H_2O) concentration was varied and the concentrations of others were kept constant. In testing the CO order, the concentrations of O_2 and H_2O were 20% and 6000 ppm respectively; testing the O_2 order, the concentrations of CO and H_2O were 1500 and 6000 ppm; testing the H_2O order, the concentrations of CO and O_2 were 1500 ppm and 20% respectively. The obtained reaction orders of CO, O_2 and H_2O over PC-CIi are −0.065, 0.27 and 0.39, respectively (Fig. 6).

The fact that reaction order of CO is about zero shows the CO concentration affect hardly the rate of CO oxidation. H_2O with a positive order (0.39) indicates that the presence of H_2O is in favor of the CO oxidation and increasing its concentration can enhance the catalytic activity of PC-CIi, which is in accordance with the result in Fig. 5. For the reaction order of O_2, Kotareva et al. reported [33] that it was 0.8 and near to first-order for the $PdCl_2$–$CuCl_2$/γ-Al_2O_3 catalyst at 27 °C, because the rate of re-oxidation of Cu^+ by gas oxygen was the rate-determining step [25]. Herein, the order of O_2 over PC-CIi is 0.27 and much smaller than 0.8. These results indicate that the surface of the catalyst is almost saturated with CO and O_2, leading to very weak dependency of the reaction rate on the gas-phase CO and O_2 concentrations. This also demonstrates that there are much more active oxygen species on the surface of PC-CIi catalyst at the reaction condition, resulting in that the rate of re-oxidation of Cu^+ by active oxygen species over PC-CIi is accelerated compared with that over PC-WI, and the difference between the re-oxidation of Cu^+ and surface reaction of adsorbed CO and the nearby oxygen is lower. We have found also that the apparent activation energy of CO oxidation over PC-CIi is much lower than that over PC-WI [31], implying that the surface active site or the rate-determining step for CO oxidation over these two catalysts may be different. At lower temperature the adsorption rate of reactant can usually exceed the rate of surface reaction. Therefore, the surface reaction between the adsorbed CO and the nearby oxygen species to form CO_2 or the re-oxidation of Pd^0 by Cu^{2+} seems to be the rate-determining step.

3.7. Catalyst characterization

3.7.1. XRD and TEM

The XRD patterns of catalysts are shown in Fig. 7. For Wacker type catalyst, the palladium species was suggested to be the active

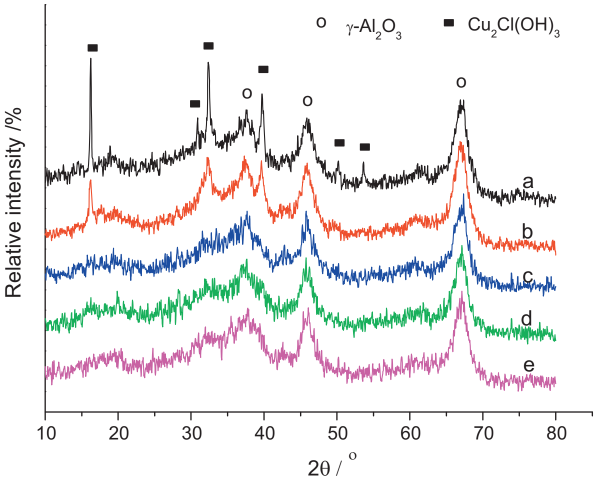

Fig. 7. XRD patterns of (a) PC-WI, (b) PC-CIw, (c) PC-CIi, (d) PC-CIa, and (e) PC-CIe.

composition [20–29], however the palladium species cannot be observed in Fig. 7, indicating that the palladium species may be highly dispersed on the surface of alumina or below detection limit of XRD.

Although the copper species is a redox partner of palladium in supported $PdCl_2$–$CuCl_2$ catalyst, it has been believed that it is closely correlated with the catalytic activity and plays a critical role in converting Pd^0 to Pd^{2+} [26,28]. Park and Lee [23] thought that the active copper phase was solid $Cu_2Cl(OH)_3$ particles, and its catalytic activity increased with an increase in the peak intensity of $Cu_2Cl(OH)_3$, which suggests that bigger crystal $Cu_2Cl(OH)_3$ particles lead to higher catalytic activity but this is unconvinced. According to the catalytic mechanism of supported $PdCl_2$–$CuCl_2$ catalyst [28,29], the step of restoring Cu^+ to Cu^{2+} by oxygen is the rate-determining step. Hence, it can be speculated that the rate of CO oxidation can be accelerated if oxidizing Cu^+ to Cu^{2+} becomes more easily and $Cu_2Cl(OH)_3$ particles highly disperse on the support surface.

The results in Fig. 7a and b show that $Cu_2Cl(OH)_3$ phase can be observed in the XRD patterns of PC-WI and PC-CIw, but $CuCl_2$ phase cannot be discerned. The crystalline sizes of $Cu_2Cl(OH)_3$ in PC-WI and PC-CIw are 34 nm and 21 nm respectively, which are calculated by the Scherrer equation based on the (1 0 1) peak of $Cu_2Cl(OH)_3$, indicating that the dispersion of copper phase on the catalyst can be improved by CI preparation method. In the XRD patterns of PC-CIa, PC-CIe, and PC-CIi, only γ-Al_2O_3 phase can be detected and any copper phase is hardly discerned, which indicates that the copper phase is highly dispersed on alumina surface or its crystalline sizes is too small to be detected by XRD technique.

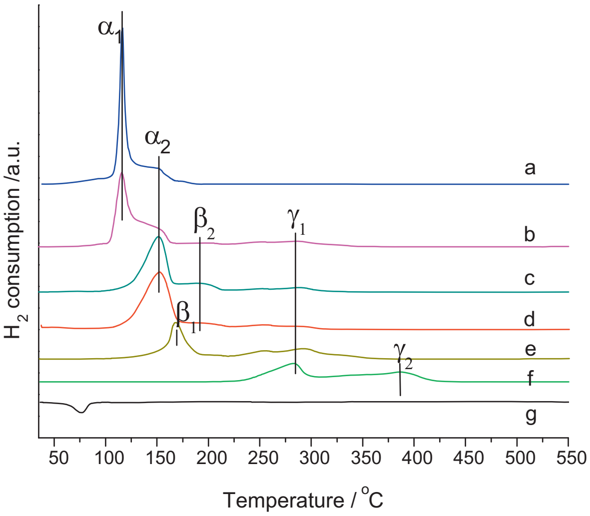

Fig. 9. TPR profiles of (a) PC-CIi, (b) PC-CIw, (c) PC-CIa, (d) PC-CIe, (e) PC-WI, (f) $CuCl_2/Al_2O_3$, and (g) $PdCl_2/Al_2O_3$. ($PdCl_2/Al_2O_3$ and $CuCl_2/Al_2O_3$ were prepared by the same method as PC-WI.)

In the TEM image (Fig. 8) of PC-CIi catalyst, some stacking of Al_2O_3 layers can be evidently observed, and the crystalline copper and palladium phase are hardly observed, indicating further the very high dispersion of copper and palladium on the support. Other PC-CI catalysts except PC-CIw were also examined by TEM (not shown), the same features as PC-CIi can be observed.

3.7.2. H_2-TPR

The TPR profiles of the $PdCl_2/Al_2O_3$, $CuCl_2/Al_2O_3$, PC-WI, and PC-CI samples are shown in Fig. 9. $PdCl_2/Al_2O_3$ shows a negative peak at ~75° (Fig. 9g), due to the decomposition of Pd β-hydride to release hydrogen [34–36], indicating that $PdCl_2/Al_2O_3$ can be reduced at room temperature in the absence of copper species. $CuCl_2/Al_2O_3$ shows two reduction peaks at ~285 °C and ~385 °C (Fig. 9f). There are also two reduction peaks in the TPR profiles of PC-WI (Fig. 9e), β_1 at ~168 °C and the broad peak γ_1 at ~285 °C. Compared with the TPR profiles of $PdCl_2/Al_2O_3$ and $CuCl_2/Al_2O_3$, the reduction peaks of copper species in PC-WI shift to lower temperature due to the presence of palladium species and the negative peak at ~75 °C disappears.

Hydrogen consumption in the reduction of PC-WI is ~615 μmol/g, more than the theoretical hydrogen consump-

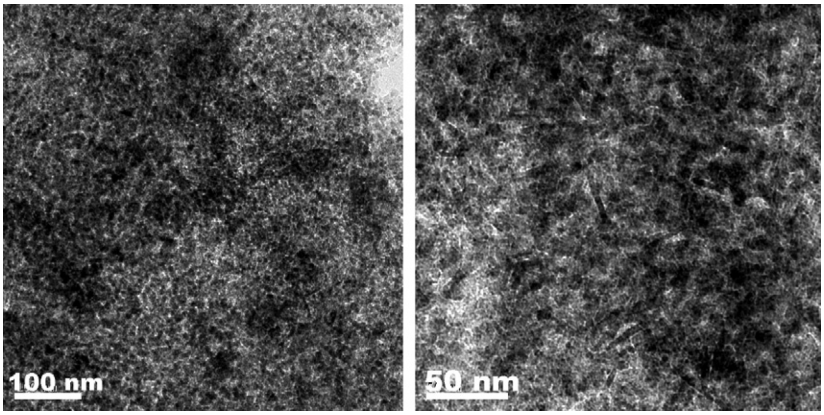

Fig. 8. TEM images of PC-CIi sample.

Table 1
Pd and Cu loadings and H_2-TPR results of the PC catalysts.

Catalyst	Pd/wt.%	Cu/wt.%	H_2 uptake/μmol/g						
			α_1	α_2	β_1	β_2	γ_1	Total	Theoretical
PC-WI	1.4	3.1	–	–	334	–	281	615	620
PC-CIi	1.2	3.2	454	167	–	–	–	621	616
PC-CIw	1.3	3.2	254	279	–	–	99	632	625
PC-CIa	1.3	3.2	–	474	–	79	75	628	625
PC-CIe	1.5	3.1	–	466	–	88	75	629	629

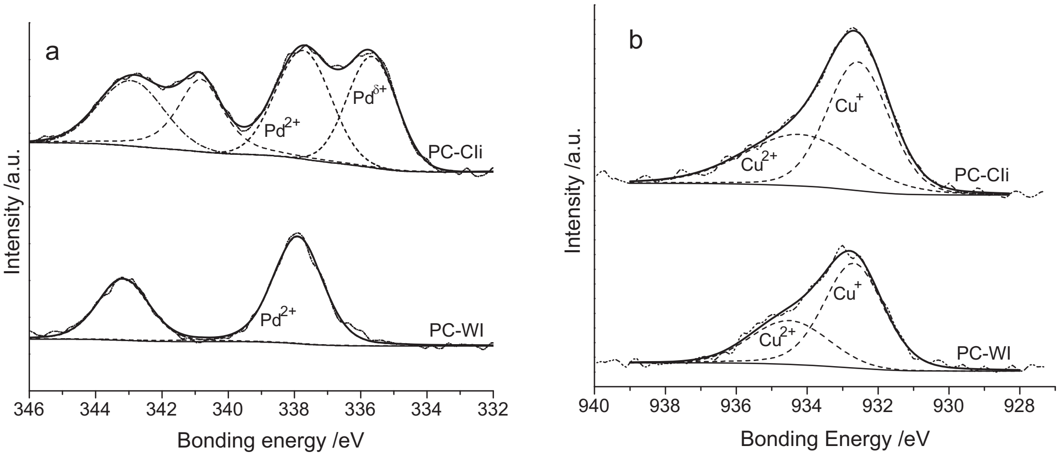

Fig. 10. (a) Pd3d and (b) Cu2p XPS spectra of PC-WI and PC-CIi.

tion in the reduction of 3.3%Cu–Cl_2/Al_2O_3 (519 μmol/g) and similar to the theoretical hydrogen consumption (620 μmol/g) for the reduction of Pd and Cu species, indicating that the peak β_1 should be ascribed to the co-reduction of palladium and copper species, which also demonstrates the interaction between palladium and copper phase. The broad peak γ_1 at ~285 °C is due to the reduction of bulk copper phase that is not interacted with palladium phase.

All PC-CI catalysts have two reduction peaks (Fig. 9a–d). Based on different peak positions and shapes, the PC-CI samples can be divided into two groups. The first group includes PC-CIa and PC-CIe, and their TPR profiles (Fig. 9c and d) are very similar, showing a main peak α_2 at ~150 °C for the co-reduction of Pd and Cu species and a broad small peak β_2 at ~192 °C for the reduction of bulk Cu phase. The second group includes PC-CIw and PC-CIi, and in their TPR profiles, there are a very sharp main peak α_1 at ~115 °C for the co-reduction of Pd and Cu phase and a broad shoulder peak α_2 at ~150 °C due to the reduction of bulk Cu phase. Compared with the α peaks of PC-CIw, the α_1 peak of PC-CIi with a H_2 consumption of 454 μmol/g is much larger and its shoulder peak α_2 is weaker. The hydrogen consumptions in the reduction of PC-CI catalysts are also very close to the theoretical hydrogen consumptions for the reduction of both Pd and Cu species (Table 1). This situation demonstrates Pd and Cu species in the PC-CI catalysts can be co-reduced by H_2.

It is evident that the reduction peaks of second group catalysts are located at lower temperature and their main reduction peaks are much stronger and sharper, especially for the PC-CIi catalyst, compared with first group catalysts. This indicates that Cu^{2+} species over second group catalysts is much easy to be reduced, indicating that the rate of the re-oxidation of Pd^0 by Cu^{2+} is faster than that over first group catalysts. Therefore, it can be concluded that the performances of the catalysts are influenced by the low temperature reducibility of Cu^{2+} species.

3.7.3. XPS

The PC-WI and PC-CIi catalysts were tested by XPS, and the results are shown in Fig. 10 and Table 2. The Pd 3d spectrum of PC-WI shows only Pd^{2+} peaks at 337.9 and 343.2 eV [34–37], which is considered to be the active Pd species for conventional $PdCl_2$–$CuCl_2$ catalyst. The Pd 3d spectrum of PC-CIi exhibits the Pd^{2+} peaks and another pare of peaks at 335.7 and 340.8 eV that is below the bonding energy of Pd^{2+} and above that of Pd^0 [34–37]. So this pair of peaks may be ascribed to $Pd^{\delta+}$ species, which may be an important factor resulting in the higher catalytic activity of PC-CIi.

The Cu 2p spectra of PC-WI and PC-CIi exhibit the Cu^+ (932.6 eV) and Cu^{2+} (934.3 eV) species [37]. The Cu^{2+} species is considered to be the active component in the $PdCl_2$–$CuCl_2$ catalyst. The relative percentages of Pd and Cu species are quantified based on the area of their XPS peaks and shown in Table 2. The results show that PC-CIi catalyst possesses much more surface active Cu and Pd species than PC-WI, therefore the higher catalytic activity of PC-CIi may also correlate with more surface active Cu and Pd species.

3.7.4. In situ DRIFTS

In situ DRIFTS technology was employed to test the surface reaction of CO adsorbed on the catalysts in different atmospheres, and the results are shown in Figs. 11–15. In these DRIFTS spectra, the absorption peaks at 2300–2400 cm^{-1} are assigned to gaseous CO_2 [4,38], the peaks at 1600–1700 cm^{-1} are due to OH groups [4,38], the strong peaks at 2126 cm^{-1} are ascribed to Cu^+–CO complex, the

Table 2
Surface composition of the catalysts calculated by the XPS data.

Catalyst	Pd^{2+}/at.%	$Pd^{\delta+}$/at.%	Cu^{2+}/at.%	Cu^+/at.%	Total Pd/at.%	Total Cu/at.%
PC-WI	0.25	0	0.33	0.69	0.25	1.02
PC-CIi	0.28	0.25	0.57	0.79	0.53	1.36

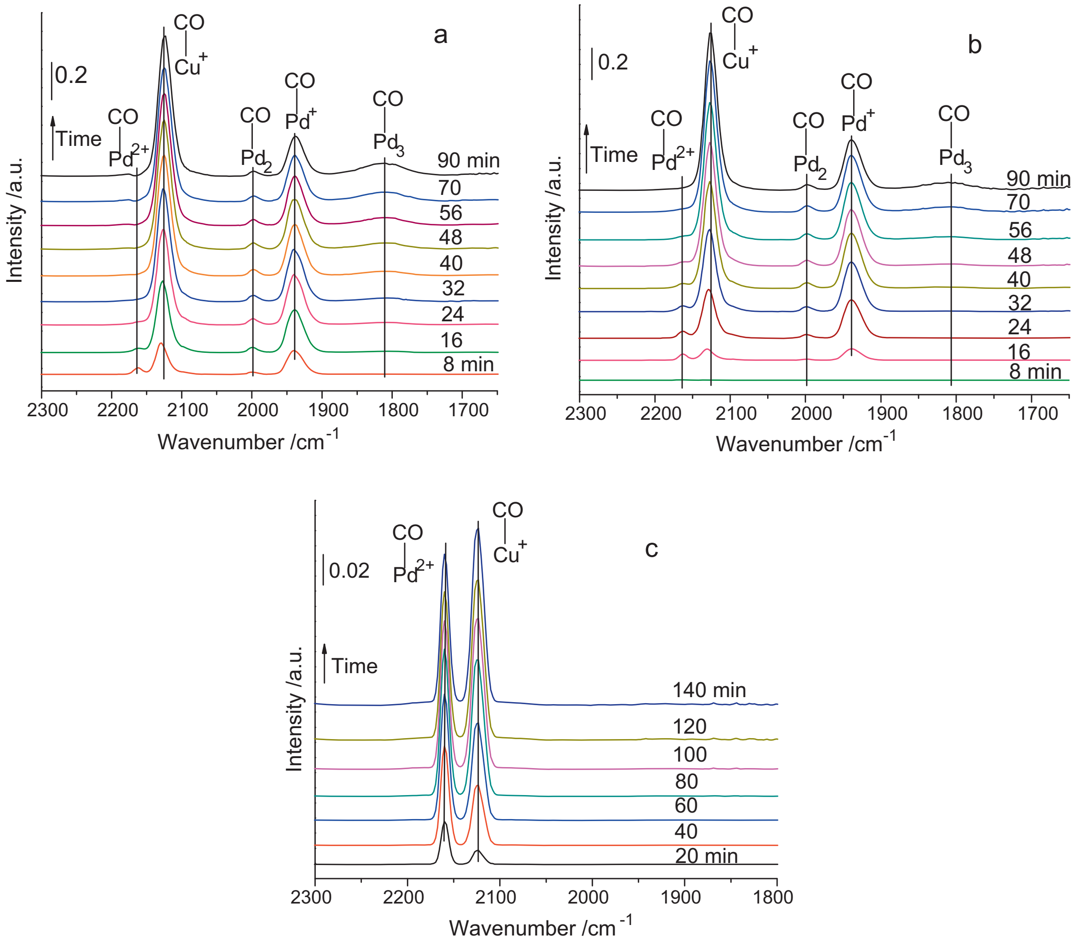

Fig. 11. *In situ* DRIFTS spectra of CO adsorbed over (a) PC-CIi, (b) PC-CIw and (c) PC-WI at 25 °C.

peaks at 2162 cm^{-1} are associated with terminal CO groups in Pd^{2+} complexes (Pd^{2+}–CO), the peaks at 1990–2000 cm^{-1} are related with bridge-bonded CO on palladium mental surfaces (Pd$_2$–CO), the peaks at 1930–1940 cm^{-1} are associated with bridged carbonyl ligands in Pd$^+$ complexes (Pd$^+$–CO) [25,28], and the broad peaks at 1810 cm^{-1} are assigned to triply bonded CO on metallic Pd (Pd$_3$–CO) [39,40].

In the DRIFTS spectra over PC-CIi catalyst (Fig. 11a), the CO adsorption peaks are located at 2162 (Pd^{2+}–CO), 2126 (Cu$^+$–CO), 1939 (Pd$^+$–CO) and 1997 cm^{-1} (Pd$_2$–CO), respectively. With an increase in the contact time, the Pd^{2+}–CO peak disappears gradually and all the other peaks retain their positions and their intensities grow obviously, and the absorption peak of Pd$_3$–CO at 1810 cm^{-1} appears gradually [39,40]. For PC-CIw catalyst, it exhibits similar DRIFTS spectra of CO adsorbed (Fig. 11b) with that of PC-CIi, however the rate of CO adsorption on PC-CIw is slight slow because it needs a little more time to reach the steady-state.

For the PC-WI catalyst, its absorption spectra of CO adsorption (Fig. 11c) are different with that on PC-CIi. Only the Pd^{2+}–CO and Cu$^+$–CO peaks can be observed, indicating that only Pd^{2+} species exists on PC-WI in accord with XPS results, and it cannot be reduced to other low valent Pd species by CO at 25 °C. Being different with PC-CIi, the peak intensity of Pd^{2+}–CO (∼2162 cm^{-1}) on PC-WI are much stronger than one on PC-CIi, showing that CO adsorbed mainly on Pd^{2+} and Cu$^+$ sites and not on Pd$^+$ sites.

Fig. 12 shows the *in situ* DRIFTS spectra of CO/O$_2$ co-adsorbed over the catalysts. For the PC-CIi catalyst, when 5% O$_2$ is added to the mixture gases of 0.15%CO/He, the Cu$^+$–CO peak decreases, because Cu$^+$ is re-oxidized to Cu^{2+} and Cu^{2+}–CO is very unstable, resulting in its CO absorption peak being hardly observed [25,28]. The absorption peaks of Pd$_2$–CO and Pd$^+$–CO increase at the expense of Pd$_3$–CO peak, because one of Pd atoms in Pd$_3$ cluster is oxidized to Pd$^+$ by Cu^{2+}, hence CO adsorbs on other two Pd atoms to form Pd$_2$–CO, resulting in an enhancement of its peak intensity. With an increase in the O$_2$ concentration, this phenomenon above becomes more distinct. For the PC-CIw catalyst (Fig. 12b), its spectra are similar to these on PC-CIi except for the larger effect of the O$_2$ concentration on the CO adsorption on PC-CIw.

For the PC-WI catalyst (Fig. 12c), the intensities of the Pd^{2+}–CO and Cu$^+$–CO peaks decrease with an increase in the O$_2$ concentration. Compared with the DRIFTS spectra over PC-CIi or PC-CIw, the peak of gas-phase CO$_2$ on PC-WI catalyst is smaller, that is to say, the amount of CO$_2$ on PC-WI catalyst is less than that on PC-CIi or PC-CIw catalyst. And the change of Cu$^+$–CO peak intensity on PC-WI is less with the change of O$_2$ amount, indicating that Cu$^+$ species on PC-WI is much harder to be re-oxidized.

Fig. 13 shows *in situ* DRIFTS spectra of CO/O$_2$/H$_2$O adsorbed over the catalysts. For the PC-CIi catalyst (Fig. 13a), when H$_2$O is introduced to the mixture gases of 0.15%CO/20%O$_2$/He, the intensity of Cu$^+$–CO peak decreases significantly. After ∼10 min, this peak almost disappears and only a small broad peak maintains, which suggests that the presence of water promote the rate of Cu$^+$ re-oxidation. The intensities of other CO related peaks simultaneously decrease with the abatement of Cu$^+$–CO peak but the peaks of gaseous CO$_2$ and OH group increase remarkably. After ∼40 min, all the peak intensities are almost no longer alterable and the Pd$^+$–CO and Pd$_3$–CO peaks still retain, which indicates that CO oxidation over PC-CIi is via Pd$^+$–CO and Pd$_3$–CO as intermediates.

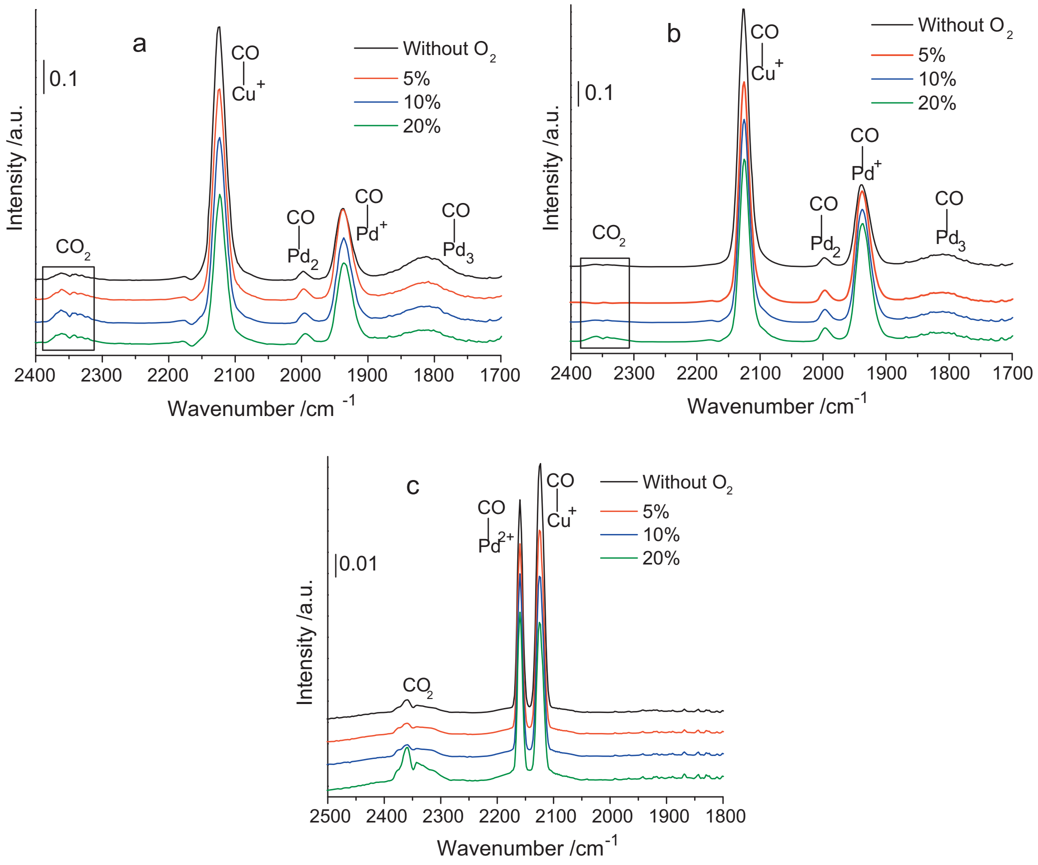

Fig. 12. *In situ* DRIFTS spectra of CO adsorbed over (a) PC-CIi, (b) PC-CIw and (c) PC-WI in the presence of O_2 with different concentrations at 25 °C.

The *in situ* DRIFTS spectra of PC-CIw (Fig. 13b) are similar to that of PC-CIi. All CO related peaks decrease quickly, and the peaks of gaseous CO_2 and OH group increase with an increase in time. However, some differences can still be found. Firstly, it needs much time to reach a steady-state, such as, after ~30 min the Cu^+–CO peak disappears, which is much slower compared with that on PC-CIi, indicating a slower rate of oxidation of Cu^+ to Cu^{2+}. It may explain the better catalytic performance of PC-CIi for CO oxidation than PC-CIw. Secondly, the peak intensity of gas CO_2 in Fig. 13b develops more slowly and seems to be weaker than that in Fig. 13a, which also suggests that the rate of CO oxidation over PC-CIw is slower than over PC-CIi.

For PC-WI (Fig. 13c), when H_2O is introduced into the mixture gases of 0.15%CO/20%O_2/He, the peak intensities of Pd^{2+}–CO and Cu^+–CO decrease and that of gas phase CO_2 increase simultaneously. After ~45 min, the spectra are almost no longer changed and the Pd^{2+}–CO and Cu^+–CO peaks still exist. Compared with the absorption peak of Pd^+–CO over PC-CIi (Fig. 13a), the intensity of Pd^{2+}–CO peak over PC-WI decreases much more slightly and slowly, indicating that CO adsorbed on Pd^+ species of PC-CIi is more easily oxidized to CO_2 compared with CO on Pd^{2+} species of PC-WI. Further this demonstrates that Pd^+ species is much more active than Pd^{2+} species for CO oxidation.

The Cu^+ species cannot be completely re-oxidized by oxygen over PC-WI because the re-oxidation of Cu^+ is the rate-determining step in the conventional $PdCl_2$–$CuCl_2$ catalyst. And the fact that the faster complete re-oxidation of Cu^+ species by oxygen over PC-CIi (Fig. 13a) reveals that the rate determining step is remarkably accelerated or changed, which is also proved by the little effect of Cu loading on the catalytic activity of PC-CIi for CO oxidation (Fig. 2b) and weaker dependency of the reaction rate on the O_2 concentrations (Fig. 6).

The results above show that, there are mainly two surface reaction steps relating to the rate-determining step over the PC-CIi catalyst: the oxidation of adsorbed CO on Pd^+ to form CO_2 and the re-oxidation of Pd^0 by Cu^{2+} to regenerate active Pd^+. In order to determine the rate-determining step in the whole catalytic cycle over PC-CIi catalyst, *in situ* DRIFT spectra in the feed of CO + O_2 + H_2O with the time of removing CO are measured, and the results are shown in Fig. 14. The results show that the intensity of the Pd^+–CO peak decreases much faster when CO is removed from the feed gas, and disappears within ~24 min, indicating that the oxidation rate of adsorbed CO on the Pd^+ active sites is much faster. The Pd_3–CO peak still retains after CO being removed for 30 min. These phenomena reveal that the re-oxidation of Pd^0 to Pd^+ by active copper species is the rate determining step for CO oxidation over PC-CIi catalyst.

3.7.5. *Discussion about the catalytic mechanism of CO oxidation*

Based on the results obtained herein and achievements reported previously [22–29], a potential reaction pathway is proposed for CO oxidation over PC-CIi catalyst as shown in Fig. 15. At first, Pd^{2+} is totally reduced by CO and H_2O to form active Pd^+ species (Fig. 11). This initial step can quickly occur to give a small amount of CO_2, but this step is not included in the real catalytic cycle because Pd^+ cannot be re-oxidized to Pd^{2+} in the catalytic reaction (Figs. 12 and 13). A small amount of formed active Pd^+ species is further reduced to Pd^0 and CO is adsorbed on three palladium atoms with the Pd_3–CO structure (Fig. 11). Then Pd^0 is re-oxidized to Pd^+ by Cu^{2+} species (Fig. 12), and Cu^{2+} is reduced to Cu^+ simultaneously. Afterwards, Cu^+ species is re-oxidized back to Cu^{2+} species by oxygen (Figs. 12 and 13) and the catalytic cycle is completed. These steps in the mechanism above-mentioned can be well proved by *in situ* DRIFTS testing, and are similar to the well-known Wacker process

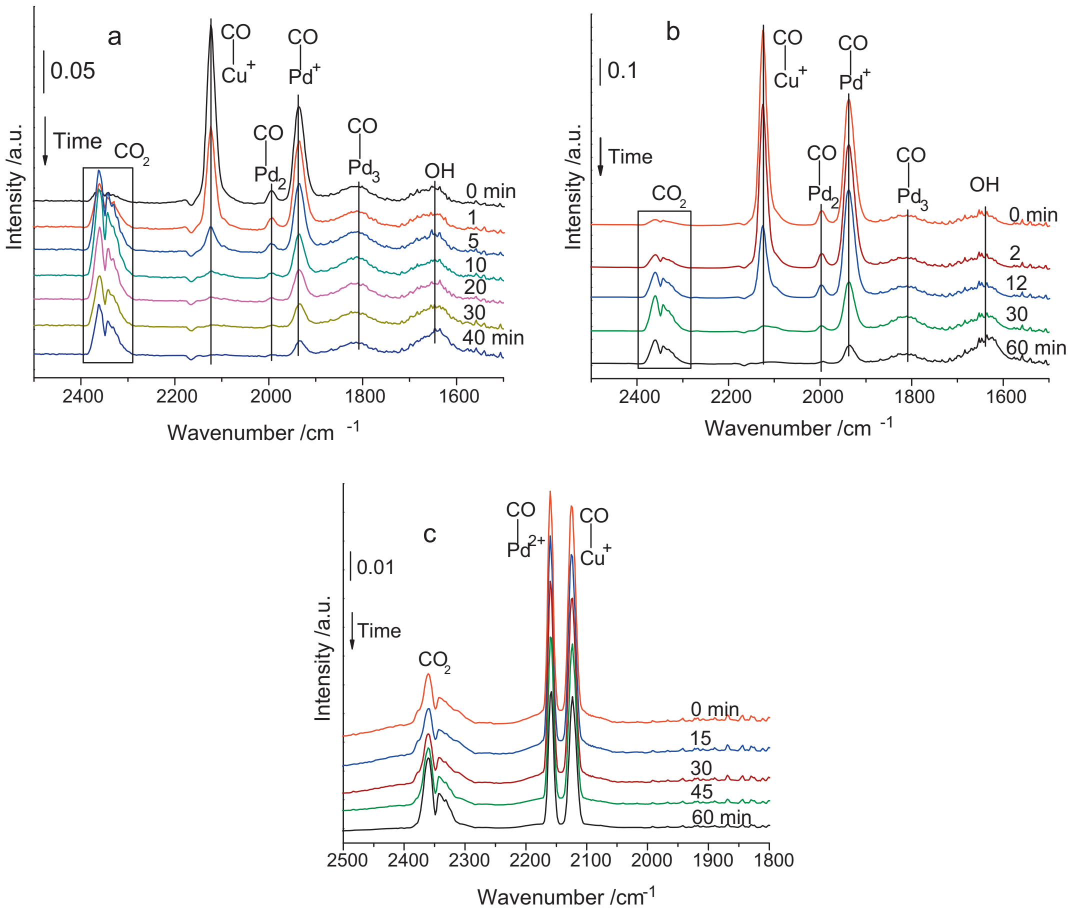

Fig. 13. *In situ* DRIFTS spectra of CO adsorbed over (a) PC-CIi, (b) PC-CIw and (c) PC-WI in the presence of 20% O_2 and ~6000 ppm H_2O at 25 °C.

over the conventional $PdCl_2$–$CuCl_2$/Al_2O_3 catalyst. However, there are still two remarkable differences between them. One is that Pd^+ is the active palladium species over the PC-CIi catalyst, and over the PC-WI catalyst Pd^{2+} is the active species. Another is that the rate-determining step (rds) of CO oxidation over the PC-CIi catalyst (Fig. 16) is Step 3 in Fig. 15, but for the PC-WI catalyst the last step (Step 4 in Fig. 15) is the rds.

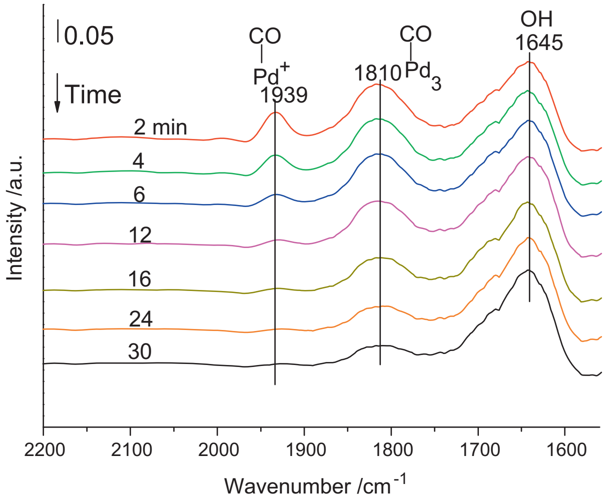

Fig. 14. *In situ* DRIFTS spectra over PC-CIi in the feed of CO + O_2 + H_2O with the time of removing CO at 25 °C.

The reasons for the high activity of PC-CIi catalyst for CO oxidation are as follows. Firstly, the adsorbed CO on Pd^+ species of PC-CIi is more easily oxidized to CO_2 compared with that on Pd^{2+} species of PC-WI (Step 2 in Fig. 15), so that Pd^+ species is more active sites than Pd^{2+} species for CO oxidation. Secondly, the Cu^{2+} species on PC-CIi catalyst has the lower-temperature reducibility (Fig. 9), resulting in the very easy reduction of Cu^{2+} (Step 3 in Fig. 15). Thirdly, the presence of moisture can make an acceleration of Cu^+ re-oxidation by oxygen, and the rate-determining step for CO oxidation over PC-CIi catalyst is the re-oxidation of Pd^0 by Cu^{2+} species as proposed

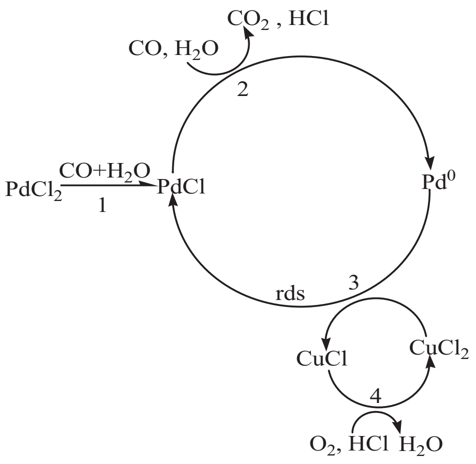

Fig. 15. Proposed catalytic CO reaction pathways over PC-CIi.

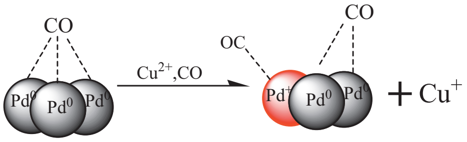

Fig. 16. Proposed the rate-determining step of CO oxidation over PC-CIi.

in Fig. 16 instead of the re-oxidation of Cu^+ by oxygen (Step 4 in Fig. 15), which is the main reason for the higher catalytic activity of PC-CIi catalyst for low temperature CO oxidation.

4. Conclusions

Using a coordination-impregnation method, the $Pd–Cu–Cl_x/Al_2O_3$ (PC-CI) catalysts were prepared and exhibited excellent catalytic activities for CO oxidation compared with the $Pd–Cu–Cl_x/Al_2O_3$ (PC-WI) catalyst prepared by wet impregnation. In the process of preparing the PC-CI catalysts, different solvents affect obviously their catalytic performance and isopropanol is the most suitable solvent among water, ethanol, acetone and isopropanol.

Over the PC-CI catalyst the CO oxidation can be enhanced remarkably with an increase in moisture concentration because the presence of moisture can prompt the rate of Cu^+ re-oxidation, but it is weakly dependent on the CO and O_2 concentrations. Compared with the PC-WI catalyst, the PC-CIi catalyst prepared by using isopropanol solvent has higher dispersion and lower-temperature reducibility of copper phase, and possesses higher active Pd^+ species and much more Cu^{2+} active species on its surface.

In the CO low-temperature oxidation catalyzed by the PC-CIi catalyst, the Cu^+ re-oxidation by oxygen can be accelerated by moisture in feed gas and the rate-determining step is the re-oxidation of Pd^0 to Pd^+ by Cu^{2+} over the PC-CIi catalyst instead of the re-oxidation of Cu^+ to Cu^{2+} by O_2 over PC-WI catalyst, which are the main reasons that the PC-CIi catalyst behaves the excellent catalytic activity for low-temperature oxidation of CO.

Acknowledgements

This project was supported financially by the National Basic Research Program of China (2010CB732300), the National Key Technologies R&D Program of China (2007BAJ03B01) and the Fundamental Research Funds for the Central Universities.

References

[1] J.Y. Luo, M. Meng, X. Li, X.G. Li, Y.Q. Zha, T.D. Hu, Y.N. Xie, J. Zhang, J. Catal. 254 (2008) 310.
[2] C. Jones, S.H. Taylor, A. Burrows, M.J. Crudace, C.J. Kiely, G.J. Hutchings, Chem. Commun. 14 (2008) 1707.
[3] M.S. Chen, D.W. Goodman, Science 306 (2004) 252.
[4] H.Q. Zhu, Z.F. Qin, W.J. Shan, W.J. Shen, J.G. Wang, J. Catal. 225 (2004) 267.
[5] D.R. Merrill, C.C. Scalione, J. Am. Chem. Soc. 43 (1921) 1982.
[6] C. Yoon, D.L. Cocke, J. Catal. 113 (1988) 267.
[7] X.W. Xie, Y. Li, Z.Q. Liu, M. Haruta, W.J. Shen, Nature 458 (2009) 746.
[8] Y.B. Yu, T. Takei, H. Ohashi, H. He, X.L. Zhang, M. Haruta, J. Catal. 267 (2009) 121.
[9] M. Haruta, N. Yamada, T. Kobayashi, S. Iijima, J. Catal. 115 (1989) 301.
[10] M. Date, M. Okumura, S. Tsubota, M. Haruta, Angew. Chem. Int. Ed. 43 (2004) 2129.
[11] S.H. Oh, G.B. Hoflund, J. Catal. 245 (2007) 35.
[12] H.G. Zhu, Z. Ma, J.C. Clark, Z.W. Pan, S.H. Overbury, S. Dai, Appl. Catal. A 326 (2007) 89.
[13] W.S. Lee, B.Z. Wan, C.N. Kuo, W.C. Lee, S.F. Cheng, Catal. Commun. 8 (2007) 1604.
[14] I.D. Gomez, I. Kocemba, J.M. Rynkowski, Appl. Catal. B 88 (2009) 83.
[15] J.M.C. Soares, M. Hall, M. Cristofolini, M. Bowker, Catal. Lett. 109 (2006) 103.
[16] D.N. Briggs, K.H. Lawrence, A.T. Bell, Appl. Catal. A 366 (2009) 71.
[17] Y. Cao, P. Yang, C.Z. Yao, N. Yi, W.L. Feng, W.L. Dai, K.N. Fan, Appl. Catal. A 272 (2004) 15.
[18] P. Yang, Y. Cao, W.L. Dai, J.F. Deng, K.N. Fan, Appl. Catal. A 243 (2003) 323.
[19] M. Okamoto, Y. Taniguchi, J. Catal. 261 (2009) 195.
[20] J.S. Lee, E.D. Park, B.J. Song, Catal. Today 54 (1999) 57.
[21] K.D. Kim, I.S. Nam, J.S. Chung, J.S. Lee, S.G. Ryu, Y.S. Yang, Appl. Catal. B 5 (1994) 103.
[22] E.D. Park, J.S. Lee, J. Catal. 193 (2000) 5.
[23] E.D. Park, J.S. Lee, J. Catal. 180 (1998) 121.
[24] C.W. Lee, S.J. Park, Y.S. Kim, P.J. Chong, Bull. Korean Chem. Soc. 16 (1995) 296.
[25] K.I. Choi, M.A. Vannice, J. Catal. 127 (1991) 489.
[26] J.S. Lee, S.H. Choi, K.D. Kim, M. Nomura, Appl. Catal. B 7 (1996) 199.
[27] S.H. Choi, J.S. Lee, React. Kinet. Catal. Lett. 57 (1996) 227.
[28] K.I. Choi, M.A. Vannice, J. Catal. 127 (1991) 465.
[29] E.D. Park, S.H. Choi, J.S. Lee, J. Phys. Chem. B 104 (2000) 5586.
[30] D.J. Koh, J.H. Song, S.W. Ham, I.S. Nam, R.W. Chang, E.D. Park, J.S. Lee, Y.G. Kim, Korean J. Chem. Eng. 14 (1997) 486.
[31] Y.X. Shen, G.Z. Lu, Y. Guo, Y.Q. Wang, Chem. Commun. 46 (2010) 8433.
[32] M.N. Desai, J.B. Butt, J.S. Dranoff, J. Catal. 79 (1983) 95.
[33] I.A. Kotareva, I.V. Oshanina, K.Y. Odintsov, L.G. Bruk, O.N. Temkin, Kinet. Catal. 49 (2008) 18.
[34] W.J. Shen, M. Okumura, Y. Matsumura, M. Haruta, Appl. Catal. A 213 (2001) 225.
[35] M.L. Cubeiro, J.L.G. Fierro, Appl. Catal. A 168 (1998) 307.
[36] N. Iwasa, N. Kudo, H. Takahashi, S. Masuda, N. Takazawa, Catal. Lett. 19 (1993) 211.
[37] C.D. Wagner, J.F. Moulder, L.E. Davis, W.M. Riggs, Handbook of X-ray Photoelectron Spectroscopy, Standard XPS Spectra of Elements. Perking-Elmer Corporation, Physical Electronics Division.
[38] H.Q. Zhu, Z.F. Qin, W.J. Shan, W.J. Shen, J.G. Wang, J. Catal. 233 (2005) 41.
[39] S.D. Ebbesen, B.L. Mojet, L. Lefferts, Phys. Chem. Chem. Phys. 11 (2009) 641.
[40] G. Rupprechter, H. Unterhalt, M. Morkel, P. Galletto, L.J. Hu, H.J. Freund, Surf. Sci. 502 (2002) 109.